PAN POLISH ACADEMY OF SCIENCES

Opto-Electronics Review

journal homepage: https://journals.pan.pl/opelre

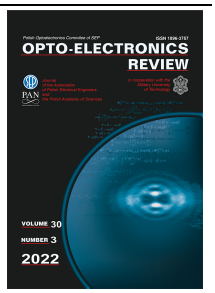

Low-pass RC filter modified by liquid crystal exhibiting one Debye relaxation - theoretical approach

Paweł J. Perkowski*

Institute of Applied Physics, Military University of Technology, 2 gen. Kaliskiego St., 00-908 Warsaw, Poland

Article info

Article history:
Received 13 Apr. 2022
Received in revised form 16 May 2022
Accepted 02 Jun. 2022
Available on-line 9 Aug. 2022

Keywords:
Liquid crystal; impedance; low-frequency filter; dielectric relaxation; permittivity.

Abstract

The solid dielectrics used in the capacitors exhibit rather high-frequency relaxations. This means that in the radio-frequency range, the capacitors exhibit a constant capacity. When liquid crystal is put into the capacitors, it is observed that in the radio-frequency range the capacity changes (decreases with frequency). This is due to the fact that liquid crystals exhibit relaxation in the radio-frequency range. In this paper, the formulas for the electric response of a low-frequency RC filter with liquid crystal characterized by complex electric permittivity are derived. One Debye-type relaxation is assumed in the calculations. The influence of strengths and relaxation time (frequency) of relaxation mode in liquid crystal on the electric response of low-frequency filters is discussed.

1. Introduction

Liquid crystal phases exhibit unique electric properties. In the radio-frequency range, they manifest different relaxations [1]. Some of them are molecular relaxations, well seen in isotropic liquid or nematic phases [2], while some are called collective modes and are well seen in smectic phases [3, 4]. Simple molecular modes are usually described by the Debye model of relaxation [5], while collective modes are usually described by more complicated models: Cole-Cole [6], Davidson-Cole [7], or Havriliak-Negami [8]. When the impedance of a measuring cell is measured with an impedance analyser, the electric properties of the measured medium, called electric permittivity (or permittivity) can be calculated. Usually, the permittivity is the complex number ε^* [9–11]. In this paper, the opposite situation is shown: when the electric properties of a liquid crystal (dispersion of its electric permittivity) can influence a simple electric circuit property: a low-frequency resistor-capacitor (RC) filter. This paper presents the electric response of a low-frequency filter numerically created for three different liquid crystals (with low, average, and high dielectric strength $\delta\varepsilon$) placed in a capacitor in an RC filter.

*Corresponding author at: pawel.perkowski@wat.edu.pl

2. RC filter with an empty capacitor

The low-pass RC filter consists of the resistance R and the capacitance C_0 of the empty capacitor serially connected (Fig. 1).

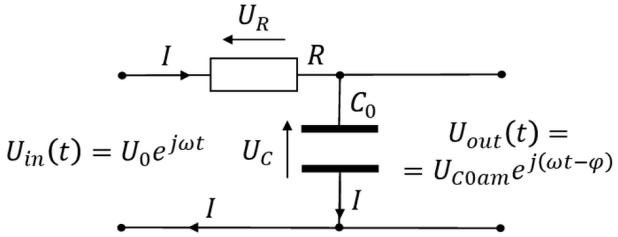

Fig. 1. The low-pass RC filter as a serial connection of the resistance R and the capacitance C_0 of the empty capacitor. In-signal $[U_{in}(t)]$ generates the current $[I(t)]$. And the current generates the out-signal $[U_{out}(t)]$.

When the differential equation (derived from the Kirchhoff second law) describing the electric charge $q(t)$ in RC_0 circuit, forced by the harmonic electric field $U_{in}(t) = U_0 e^{j\omega t}$:

$$\frac{dq}{dt} + \omega_{RC} q = \frac{U_0}{R} e^{j\omega t}, \tag{1}$$

https://doi.org/10.24425/opelre.2022.141949
1896-3757/ Association of Polish Electrical Engineers (SEP) and Polish Academy of Sciences (PAS). Published by PAS

where $\omega_{RC} = \frac{1}{RC_0}$ stands for the cut-off angular frequency of RC_0 circuit, is analysed, then the stationary solution $q(t)$ takes the following form:

$$q(t) = U_0 e^{j\omega t} C_0 \left(\frac{1}{1+\Omega_{RC}^2} - j\frac{\Omega_{RC}}{1+\Omega_{RC}^2} \right) = U_0 e^{j\omega t} C_0 (\varepsilon'_{RC} - j\varepsilon''_{RC}) = U_0 e^{j\omega t} C, \quad (2)$$

where coefficient $\Omega_{RC} = \frac{\omega}{\omega_{RC}}$ is the frequency normalized to the cut-off frequency ω_{RC} of RC_0 circuit.

Analysing (2), it can be concluded that the capacitor C_0 together with the resistor R behave as a "complex" capacitance of $C = C_0(\varepsilon'_{RC} - j\varepsilon''_{RC}) = C_0 \left(\frac{1}{1+\Omega_{RC}^2} - j\frac{\Omega_{RC}}{1+\Omega_{RC}^2} \right)$.

When the resistor R is small, then ω_{RC} goes to infinity, Ω_{RC} goes to zero, and C is close to C_0 (low-frequency capacitance limit). When R exhibits a limit value, for high frequencies, the effective capacitance C disappears because ω_{RC} becomes a limit value, and Ω_{RC} goes up. It means that the effective capacitor C does not work properly at high frequencies and no charge can be seen on the capacitor at high frequencies. The capacitor becomes a shortcut for high frequencies. Knowing ε'_{RC} and ε''_{RC} from the measurement, the cut-off angular frequency ω_{RC} of RC_0 circuit can be found. Both the parameters ε'_{RC} and ε''_{RC} have nothing to do with the electric permittivity. These are the parameters describing the RC_0 circuit.

It is known that the impedance analyser measures the current $I(t)$ as the result of applying the electric harmonic voltage $U_0 e^{j\omega t}$. To calculate this current, both sides of (2) should be differentiated:

$$\begin{aligned} I(t) &= \frac{d}{dt} q(t) = \frac{d}{dt} U_0 e^{j\omega t} C_0 \left(\frac{1}{1+\Omega_{RC}^2} - j\frac{\Omega_{RC}}{1+\Omega_{RC}^2} \right) \\ &= j\omega U_0 e^{j\omega t} C_0 (\varepsilon'_{RC} - j\varepsilon''_{RC}) \\ &= \varepsilon'_{RC} \omega C_0 U_0 e^{j\left(\omega t + \frac{\pi}{2}\right)} - j\varepsilon''_{RC} \omega C_0 U_0 j e^{j\omega t} U_0 e^{j\omega t} \\ &= \varepsilon'_{RC} \omega C_0 U_0 e^{j\left(\omega t + \frac{\pi}{2}\right)} + \varepsilon''_{RC} \omega C_0 U_0 e^{j\omega t}. \end{aligned} \quad (3)$$

The first part of the current $I(t)$ leads the AC voltage by $\frac{\pi}{2}$ rad, while the second part of the current $I(t)$ is in phase with the electric voltage.

When the current $I(t)$ and impedance of the capacitor $X_{C0} = -j\frac{1}{\omega C_0}$ are multiplied, the electric voltage $U_{out}(t)$ on the capacitor (*vs.* time) is obtained:

$$\begin{aligned} U_{out}(t) &= I(t) \cdot X_{C0} \\ &= \left(\varepsilon'_{RC} \omega C_0 U_0 e^{j\left(\omega t + \frac{\pi}{2}\right)} + \varepsilon''_{RC} \omega C_0 U_0 e^{j\omega t} \right) \left(-j\frac{1}{\omega C_0} \right) \\ &= \left(\varepsilon'_{RC} \omega C_0 U_0 e^{j\left(\omega t + \frac{\pi}{2}\right)} + \varepsilon''_{RC} \omega C_0 U_0 e^{j\omega t} \right) \left(\frac{1}{\omega C_0} e^{-j\frac{\pi}{2}} \right) \\ &= \varepsilon'_{RC} U_0 e^{j\left(\omega t + \frac{\pi}{2}\right)} e^{-j\frac{\pi}{2}} + \varepsilon''_{RC} U_0 e^{j\omega t} e^{-j\frac{\pi}{2}} \\ &= \varepsilon'_{RC} U_0 e^{j\omega t} + \varepsilon''_{RC} U_0 e^{j\left(\omega t - \frac{\pi}{2}\right)} \\ &= \frac{1}{1+\Omega_{RC}^2} U_0 e^{j\omega t} + \frac{\Omega_{RC}}{1+\Omega_{RC}^2} U_0 e^{j\left(\omega t - \frac{\pi}{2}\right)} = \\ &= U_{C0(0)} e^{j\omega t} + U_{C0\left(-\frac{\pi}{2}\right)} e^{j\left(\omega t - \frac{\pi}{2}\right)}. \end{aligned} \quad (4)$$

It is seen that the first part $[U_{C0(0)}]$ of (4) is in phase with the in-signal, while the second part $[U_{C0\left(-\frac{\pi}{2}\right)}]$ lags the in-signal by $\frac{\pi}{2}$. Equation (4) can be expressed as a function of the angular frequency ω:

$$\begin{aligned} U_{out}(t) &= U_0 e^{j\omega t} \left(\frac{1}{1+\left(\frac{\omega}{\omega_{RC}}\right)^2} + \frac{\frac{\omega}{\omega_{RC}}}{1+\left(\frac{\omega}{\omega_{RC}}\right)^2} e^{-j\frac{\pi}{2}} \right) \\ &= U_0 e^{j\omega t} \left(\frac{1}{1+\left(\frac{\omega}{\omega_{RC}}\right)^2} - \frac{\frac{\omega}{\omega_{RC}}}{1+\left(\frac{\omega}{\omega_{RC}}\right)^2} e^{+j\frac{\pi}{2}} \right). \end{aligned} \quad (5)$$

Equation (5) can be rewritten by finding the amplitude of U_{C0am} and the phase shift φ:

$$\begin{aligned} U_{out}(t) &= U_0 e^{j(\omega t - \varphi)} \sqrt{\left(\frac{1}{1+\left(\frac{\omega}{\omega_{RC}}\right)^2} \right)^2 + \left(\frac{\frac{\omega}{\omega_{RC}}}{1+\left(\frac{\omega}{\omega_{RC}}\right)^2} \right)^2} \\ &= U_0 \sqrt{\frac{1+\left(\frac{\omega}{\omega_{RC}}\right)^2}{\left(1+\left(\frac{\omega}{\omega_{RC}}\right)^2\right)^2}} e^{j(\omega t - \varphi)} = U_{C0am} e^{j(\omega t - \varphi)}, \end{aligned} \quad (6)$$

where $U_{C0am} = \frac{U_0}{\sqrt{1+\left(\frac{\omega}{\omega_{RC}}\right)^2}}$ is the amplitude of out-signal while $\sin\varphi = \frac{\frac{\omega}{\omega_{RC}}}{1+\left(\frac{\omega}{\omega_{RC}}\right)^2} \sqrt{1+\left(\frac{\omega}{\omega_{RC}}\right)^2} = \frac{\frac{\omega}{\omega_{RC}}}{\sqrt{1+\left(\frac{\omega}{\omega_{RC}}\right)^2}}$ defines the phase shift of out-signal.

In Fig. 2, the amplitude U_{C0am} of out-signal is shown, while in Fig. 3, the normalised phase shift φ/π for low-pass RC filter *vs.* angular frequency is presented. It is seen that the amplitude of the out-signal U_{C0am}, as well as the phase shift φ depend on the angular frequency ω. When the frequency is low ($\frac{\omega}{\omega_{RC}} \to 0$), then the amplitude of the out-voltage is the same as the amplitude of the in-voltage ($U_{C0am} \to U_0$). The phase shift is $\varphi \to 0$. When $\frac{\omega}{\omega_{RC}} = 1$, then $U_{C0am} = \frac{U_0}{\sqrt{2}}$ and the phase shift is $\varphi = \frac{\pi}{4}$ rad. When $\frac{\omega}{\omega_{RC}} \to \infty$, then $U_{C0am} \to 0$ and at the same time $\varphi \to \frac{\pi}{2}$ rad.

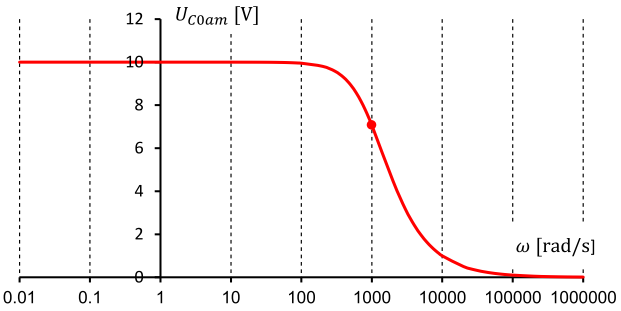

Fig. 2. Amplitude U_{C0am} of out-signal for low-pass RC filter *vs.* angular frequency ($U_0 = 10$ V, $\omega_{RC} = 1000$ rad/s).

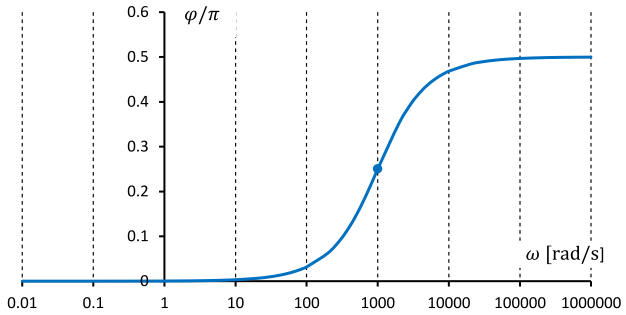

Fig. 3. Normalised phase shift φ/π for low-pass RC filter *vs.* angular frequency ($U_0 = 10$ V, $\omega_{RC} = 1000$ rad/s).

In Fig. 4, the in-phase component $[U_{C0(0)}]$ of the voltage $[U_{out}(t)]$ on the capacitor C_0 is presented. It can be seen that at $\omega_{RC} = 1000$ rad/s: $U_{C0(0)} = \frac{1}{2}U_0$. In Fig. 5, $-\frac{\pi}{2}$ shifted component $[U_{C0\left(-\frac{\pi}{2}\right)}]$ of the voltage $[U_{out}(t)]$ on the capacitor C_0 is presented. It can be concluded that at $\omega_{RC} = 1000$ rad/s $U_{C0\left(-\frac{\pi}{2}\right)} = \frac{1}{2}U_0$. In Fig. 6, the Cole-Cole plot for $U_{C0\left(-\frac{\pi}{2}\right)}$ *vs.* $U_{C0(0)}$ is shown. It is seen how the electric voltage U_{out} on the capacitor C_0 changes and how the phase shift φ changes with the angular frequency.

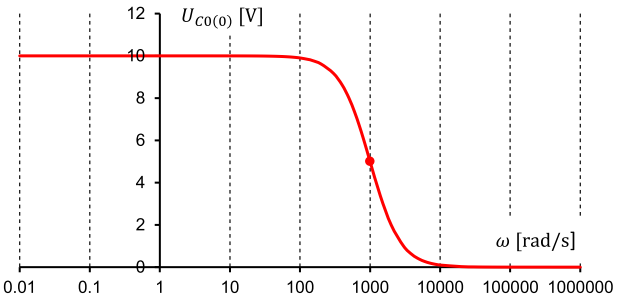

Fig. 4. In-phase component $[U_{C0(0)}]$ of voltage U_{C0} on empty capacitor C_0 ($U_0 = 10$ V, $\omega_{RC} = 1000$ rad/s) *vs.* angular frequency ω.

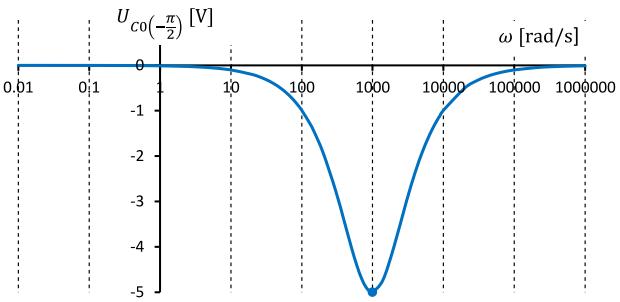

Fig. 5. $-\frac{\pi}{2}$-shifted component $[U_{C0\left(-\frac{\pi}{2}\right)}]$ of voltage U_{C0} on empty capacitor C_0 ($U_0 = 10$ V, $\omega_{RC} = 1000$ rad/s) *vs.*

3. RC filter with the capacitor filled with the liquid crystal

When the liquid crystal (LC) is placed inside the capacitor (Fig. 7), then the electric response of the RC circuit changes in comparison with the response of the RC_0 circuit.

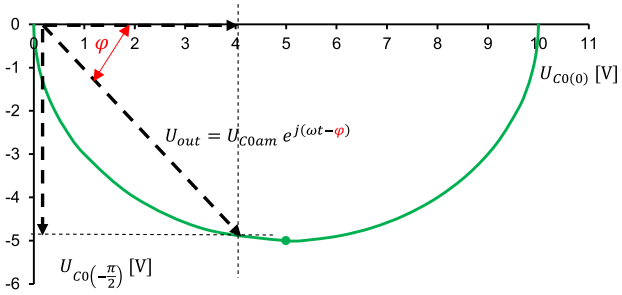

Fig. 6. $-\frac{\pi}{2}$-shifted component $[U_{C0\left(-\frac{\pi}{2}\right)}]$ *vs.* in-phase component $[U_{C0(0)}]$ on empty capacitor C_0 ($U_0 = 10$ V, $\omega_{RC} = 1000$ rad/s) – the Cole-Cole plot. The amplitude U_{C0am}, as well as the shift-angle φ are shown.

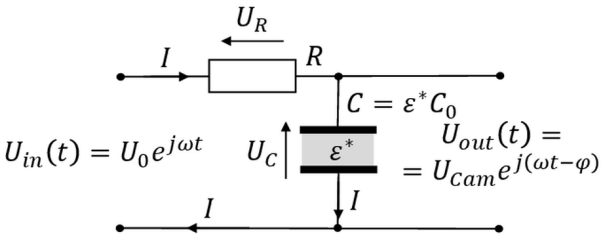

Fig. 7. Low-pass RC filter consists of the resistance R and the capacitor C filed with the LC characterized by complex permittivity: $\varepsilon^* = \varepsilon' - j\varepsilon''$. In-signal $[U_{in}(t)]$ generates the current $[I(t)]$. And the current generates the out-signal $[U_{out}(t)]$.

To solve this problem, the solution of the differential equation describing the charge $q(t)$ in the RC circuit when the capacitor is filled with a liquid crystal characterized by the complex permittivity $\varepsilon^* = \varepsilon' - j\varepsilon''$:

$$\frac{dq}{dt} + \omega_{RC}{}^* q = \frac{U_0}{R} e^{j\omega t} \tag{7}$$

should be found. In (7), $\omega_{RC}^* = \frac{\omega_{RC}}{\varepsilon^*} = \frac{1}{\varepsilon^* RC_0}$ stands for the complex relaxation angular frequency of the RC circuit.

The solution of this differential equation expresses the charge $q(t)$ as a time function :

$$q(t) = U_0 e^{j\omega t} C_0 \left(\frac{\psi'}{\psi'^2 + (\Omega_{RC} + \psi'')^2} - j\,\frac{\Omega_{RC} + \psi''}{\psi'^2 + (\Omega_{RC} + \psi'')^2} \right) = U_0 e^{j\omega t} C_0 (\varepsilon'_{EF} - j\,\varepsilon''_{EF}), \tag{8}$$

where $\psi' = \frac{\varepsilon'}{\varepsilon'^2 + \varepsilon''^2} = \frac{\varepsilon'}{|\varepsilon^*|^2}$, while $\psi'' = \frac{\varepsilon''}{\varepsilon'^2 + \varepsilon''^2} = \frac{\varepsilon''}{|\varepsilon^*|^2}$ and $\Omega_{RC} = \frac{\omega}{\omega_{RC}}$. When the cell is considered empty, then (8) modifies into the shape of (2):

$$q(t) = U_0 e^{j\omega t} C_0 \left(\frac{1}{1 + \Omega_{RC}^2} - j\,\frac{\Omega_{RC}}{1 + \Omega_{RC}^2} \right).$$

It should be remembered that the impedance analyser measures the current $I(t)$ as a result of applying the electric harmonic voltage $U_0 e^{j\omega t}$. To calculate this current, both

sides of (8) should be differentiated. The following formula for the current is derived:

$$I(t) = \frac{d}{dt}q(t) = \frac{d}{dt}U_0 e^{j\omega t} C_0 \left(\frac{\psi'}{\psi'^2 + (\Omega_{RC} + \psi'')^2} - j\,\frac{\Omega_{RC} + \psi''}{\psi'^2 + (\Omega_{RC} + \psi'')^2} \right) = j\omega U_0 e^{j\omega t} C_0 (\varepsilon'_{EF} - j\,\varepsilon''_{EF})$$
$$= \varepsilon'_{EF}\omega C_0 U_0 e^{j\left(\omega t + \frac{\pi}{2}\right)} - j\varepsilon''_{EF}\omega C_0 U_0 j e^{j\omega t}$$
$$= \varepsilon'_{EF}\omega C_0 U_0 e^{j\left(\omega t + \frac{\pi}{2}\right)} + \varepsilon''_{EF}\omega C_0 U_0 e^{j\omega t}\,. \tag{9}$$

The first part of the current $I(t)$ leads the AC voltage by $\frac{\pi}{2}$ rad, while the second part of the current $I(t)$ is in phase with the electric voltage.

When the current $I(t)$ and the impedance of the capacitor $X_C = -j\frac{1}{\omega\varepsilon^* C_0}$ are multiplied, the electric voltage $U_{out}(t)$ on the capacitor (*vs*. time) is calculated:

$$U_{out}(t) = I(t)\cdot X_C$$
$$= \left(\varepsilon'_{EF}\omega C_0 U_0 e^{j\left(\omega t + \frac{\pi}{2}\right)} + \varepsilon''_{EF}\omega C_0 U_0 e^{j\omega t}\right)\left(-j\frac{1}{\omega\varepsilon^* C_0}\right)$$
$$= \left(\varepsilon'_{EF}\omega C_0 U_0 e^{j\left(\omega t + \frac{\pi}{2}\right)} + \varepsilon''_{EF}\omega C_0 U_0 e^{j\omega t}\right)\left(-j\frac{1}{\omega(\varepsilon' - j\varepsilon'')C_0}\right)$$
$$= -jU_0\left(\frac{\psi'}{\psi'^2 + (\Omega_{RC} + \psi'')^2} e^{j\left(\omega t + \frac{\pi}{2}\right)} + \frac{\Omega_{RC} + \psi''}{\psi'^2 + (\Omega_{RC} + \psi'')^2} e^{j\omega t}\right)\left(\frac{\varepsilon'}{\varepsilon'^2 + \varepsilon''^2} + j\frac{\varepsilon''}{\varepsilon'^2 + \varepsilon''^2}\right)$$
$$= -jU_0\left(\frac{\psi'}{\psi'^2 + (\Omega_{RC} + \psi'')^2} e^{j\left(\omega t + \frac{\pi}{2}\right)} + \frac{\Omega_{RC} + \psi''}{\psi'^2 + (\Omega_{RC} + \psi'')^2} e^{j\omega t}\right)(\psi' + j\psi''), \tag{10}$$

where $\psi' = \frac{\varepsilon'}{\varepsilon'^2 + \varepsilon''^2}$ and $\psi'' = \frac{\varepsilon''}{\varepsilon'^2 + \varepsilon''^2}$.

After multiplication in (10):

$$U_{out}(t)$$
$$= -jU_0\left[\left(\frac{\psi'\psi'}{\psi'^2 + (\Omega_{RC} + \psi'')^2} e^{j\left(\omega t + \frac{\pi}{2}\right)} + \frac{(\Omega_{RC} + \psi'')\psi'}{\psi'^2 + (\Omega_{RC} + \psi'')^2} e^{j\omega t}\right) + \left(\frac{\psi' j\psi''}{\psi'^2 + (\Omega_{RC} + \psi'')^2} e^{j\left(\omega t + \frac{\pi}{2}\right)} + \frac{(\Omega_{RC} + \psi'')j\psi''}{\psi'^2 + (\Omega_{RC} + \psi'')^2} e^{j\omega t}\right)\right]$$
$$= e^{-j\frac{\pi}{2}} U_0 e^{j\omega t}\left(\frac{\psi'\psi''}{\psi'^2 + (\Omega_{RC} + \psi'')^2} e^{j\pi} + \frac{\psi'\psi' + (\Omega_{RC} + \psi'')\psi''}{\psi'^2 + (\Omega_{RC} + \psi'')^2} e^{j\frac{\pi}{2}} + \frac{(\Omega_{RC} + \psi'')\psi'}{\psi'^2 + (\Omega_{RC} + \psi'')^2}\right)$$
$$= U_0 e^{j\omega t}\left(\frac{\psi'\psi''}{\psi'^2 + (\Omega_{RC} + \psi'')^2} e^{j\pi} e^{-j\frac{\pi}{2}} + \frac{\psi'\psi' + (\Omega_{RC} + \psi'')\psi''}{\psi'^2 + (\Omega_{RC} + \psi'')^2} e^{j\frac{\pi}{2}} e^{-j\frac{\pi}{2}} + \frac{(\Omega_{RC} + \psi'')\psi'}{\psi'^2 + (\Omega_{RC} + \psi'')^2} e^{-j\frac{\pi}{2}}\right) =$$
$$= U_0 e^{j\omega t}\left(\frac{\psi'\psi''}{\psi'^2 + (\Omega_{RC} + \psi'')^2} e^{j\frac{\pi}{2}} + \frac{\psi'\psi' + (\Omega_{RC} + \psi'')\psi''}{\psi'^2 + (\Omega_{RC} + \psi'')^2} + \frac{(\Omega_{RC} + \psi'')\psi'}{\psi'^2 + (\Omega_{RC} + \psi'')^2} e^{-j\frac{\pi}{2}}\right) = U_0 e^{j\omega t}\left(\frac{\psi'\psi' + (\Omega_{RC} + \psi'')\psi''}{\psi'^2 + (\Omega_{RC} + \psi'')^2} + \frac{\psi'\psi''}{\psi'^2 + (\Omega_{RC} + \psi'')^2} e^{j\frac{\pi}{2}} - \frac{(\Omega_{RC} + \psi'')\psi'}{\psi'^2 + (\Omega_{RC} + \psi'')^2} e^{j\frac{\pi}{2}}\right)$$
$$= U_0 e^{j\omega t}\left(\frac{\psi'\psi' + (\Omega_{RC} + \psi'')\psi''}{\psi'^2 + (\Omega_{RC} + \psi'')^2} + \frac{\psi'\psi'' - (\Omega_{RC} + \psi'')\psi'}{\psi'^2 + (\Omega_{RC} + \psi'')^2} e^{+j\frac{\pi}{2}}\right)$$
$$= U_0 e^{j\omega t}\left(\frac{\psi'\psi' + (\Omega_{RC} + \psi'')\psi''}{\psi'^2 + (\Omega_{RC} + \psi'')^2} + \frac{\Omega_{RC}\psi'}{\psi'^2 + (\Omega_{RC} + \psi'')^2} e^{-j\frac{\pi}{2}}\right)$$
$$= U_0 e^{j\omega t}\left(U_{C(0)} + U_{C\left(-\frac{\pi}{2}\right)} e^{-j\frac{\pi}{2}}\right). \tag{11}$$

It is seen that the first part $[U_{C(0)}]$ of the solution $U_{out}(t)$ is in phase with the in-signal, while the second part $[U_{C\left(-\frac{\pi}{2}\right)}]$ lags the in-signal by $\frac{\pi}{2}$ rad.

If no relaxation is assumed in the liquid crystal placed inside the capacitor ($\psi'' = 0$, $\psi' = \text{const}$), then the output signal (11) takes the following form:

$$U_{out}(t)$$
$$= U_0 e^{j\omega t}\left(\frac{\psi'\psi' + (\Omega_{RC} + 0)0}{\psi'^2 + (\Omega_{RC} + 0)^2} + \frac{\Omega_{RC}\psi'}{\psi'^2 + (\Omega_{RC} + 0)^2} e^{-j\frac{\pi}{2}}\right)$$
$$= U_0 e^{j\omega t}\left(\frac{\psi'\psi'}{\psi'^2 + {\Omega_{RC}}^2} + \frac{\Omega_{RC}\psi'}{\psi'^2 + {\Omega_{RC}}^2} e^{-j\frac{\pi}{2}}\right)$$
$$= U_0 e^{j\omega t}\left(\frac{\psi'\psi'}{\psi'^2 + {\Omega_{RC}}^2} + \frac{\Omega_{RC}\psi'}{\psi'^2 + {\Omega_{RC}}^2} e^{-j\frac{\pi}{2}}\right). \tag{12}$$

In this case: $\psi' = \frac{1}{\varepsilon'}$. After the multiplication of nominators and denominators by ε'^2, one can obtain:

$$U_{out}(t) = U_0 e^{j\omega t}\left(\frac{\frac{1}{\varepsilon'^2}}{\frac{1}{\varepsilon'^2} + {\Omega_{RC}}^2} + \frac{\Omega_{RC}\,\frac{1}{\varepsilon'}}{\frac{1}{\varepsilon'^2} + {\Omega_{RC}}^2} e^{-j\frac{\pi}{2}}\right)$$
$$= U_0 e^{j\omega t}\left(\frac{1}{1 + \left(\frac{\varepsilon'\omega}{\omega_{RC}}\right)^2} + \frac{\frac{\varepsilon'\omega}{\omega_{RC}}}{1 + \left(\frac{\varepsilon'\omega}{\omega_{RC}}\right)^2} e^{-j\frac{\pi}{2}}\right). \tag{13}$$

If the amplitude/phase formula for $U_{out}(t)$ is considered, (13) can be rewritten:

$$U_{out}(t) = U_0 e^{j(\omega t - \varphi)}\sqrt{\left(\frac{1}{1 + \left(\frac{\varepsilon'\omega}{\omega_{RC}}\right)^2}\right)^2 + \left(\frac{\frac{\varepsilon'\omega}{\omega_{RC}}}{1 + \left(\frac{\varepsilon'\omega}{\omega_{RC}}\right)^2}\right)^2}$$
$$= U_0 e^{j(\omega t - \varphi)}\sqrt{\frac{1 + \left(\frac{\varepsilon'\omega}{\omega_{RC}}\right)^2}{\left(1 + \left(\frac{\varepsilon'\omega}{\omega_{RC}}\right)^2\right)^2}} = U_{Cam} e^{j(\omega t - \varphi)}\,, \tag{14}$$

where $U_{Cam} = \frac{U_0}{\sqrt{1+\left(\frac{\varepsilon'\omega}{\omega_{RC}}\right)^2}} = \frac{U_0}{\sqrt{1+(\varepsilon'\Omega_{RC})^2}}$ and

$$\sin\varphi = \frac{\frac{\varepsilon'\omega}{\omega_{RC}}}{\sqrt{1+\left(\frac{\varepsilon'\omega}{\omega_{RC}}\right)^2}} = \frac{\varepsilon'\Omega_{RC}}{\sqrt{1+(\varepsilon'\Omega_{RC})^2}}.$$

When (14) is compared with (6), true for the empty capacitor, it can be concluded that the maximum amplitude (U_0) is the same as for the empty capacitor, while the electric response for the capacitor with LC is shifted left in comparison with the empty capacitor response. The voltage $U_{out}(t)$ on the capacitor lags AC external voltage $U_0 e^{j\omega t}$ by the phase φ and this phase shift depends on the angular frequency (ω) and the electric properties (ε') of LC.

Let us think about the general case when the LC exhibits relaxation close to the cut-off frequency of RC filter. Analysing (11):

$$U_{out}(t)=U_0 e^{j\omega t}\left(\frac{\psi'\psi'+(\Omega_{RC}+\psi'')\psi''}{\psi'^2+(\Omega_{RC}+\psi'')^2}+\frac{\Omega_{RC}\psi'}{\psi'^2+(\Omega_{RC}+\psi'')^2}e^{-j\frac{\pi}{2}}\right),$$

it can be noticed that in the out-signal $U_{out}(t)$, there are two parts: part $[\frac{\psi'\psi'+(\Omega_{RC}+\psi'')\psi''}{\psi'^2+(\Omega_{RC}+\psi'')^2}]$ in phase with in-signal and part $[\frac{\Omega_{RC}\psi'}{\psi'^2+(\Omega_{RC}+\psi'')^2}]$ which lags in-signal by $\frac{\pi}{2}$ rad. This formula can be rewritten in another way:

$$\begin{aligned} U_{out}(t) &= U_0 e^{j(\omega t-\varphi)}\sqrt{\left(\frac{\psi'\psi'+(\Omega_{RC}+\psi'')\psi''}{\psi'^2+(\Omega_{RC}+\psi'')^2}\right)^2+\left(\frac{\Omega_{RC}\psi'}{\psi'^2+(\Omega_{RC}+\psi'')^2}\right)^2} \\ &= U_0\frac{\sqrt{(\psi'\psi'+(\Omega_{RC}+\psi'')\psi'')^2+(\Omega_{RC}\psi')^2}}{\psi'^2+(\Omega_{RC}+\psi'')^2}e^{j(\omega t-\varphi)} \\ &= U_{Cam}e^{j(\omega t-\varphi)}, \end{aligned} \quad (15)$$

where $U_{Cam} = U_0\frac{\sqrt{(\psi'\psi'+(\Omega_{RC}+\psi'')\psi'')^2+(\Omega_{RC}\psi')^2}}{\psi'^2+(\Omega_{RC}+\psi'')^2}$ is the amplitude of the out-signal, while $\sin\varphi = \frac{\Omega_{RC}\psi'}{\sqrt{(\psi'\psi'+(\Omega_{RC}+\psi'')\psi'')^2+(\Omega_{RC}\psi')^2}}$ describes the phase shift of the out-signal.

Equations (15) for $U_{out}(t)$, U_{Cam}, and $\sin\varphi$ are derived and true for any electric properties of LC which can be potentially put into the capacitor. Equations (15) transform into (6) when the empty capacitor is considered, and transform into (14) when the capacitor, filled with LC not showing relaxation, is considered.

Let us now consider the nematic LC which exhibits one relaxation described by the Debye model [5], and its permittivity (*vs*. angular frequency) can be calculated using the formula:

$$\begin{aligned} \varepsilon^*(\omega) &= \varepsilon_\infty + \frac{\varepsilon_S-\varepsilon_\infty}{1+j\omega\tau} \\ &= \left(\varepsilon_\infty+\frac{\varepsilon_S-\varepsilon_\infty}{1+\omega^2\tau^2}\right)-j\left(\frac{\varepsilon_S-\varepsilon_\infty}{1+\omega^2\tau^2}\omega\tau\right) = \varepsilon'-j\varepsilon'', \end{aligned} \quad (16)$$

where ε_∞ is the high-frequency limit of permittivity, ε_S is the low-frequency limit of permittivity, τ is the relaxation time of the Debye mode. The typical spectrum of permittivity is shown in Fig. 8. To calculate it from (16),

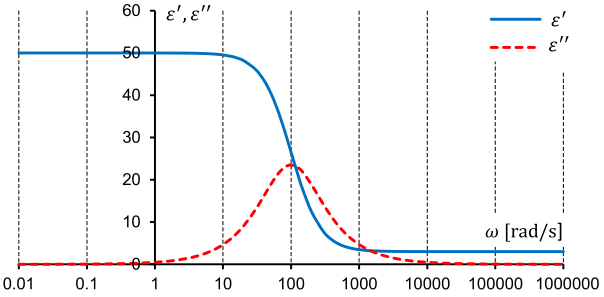

Fig. 8. Real (ε') and imaginary (ε'') parts of permittivity of liquid crystal calculated from the Debye model (16) using the following parameters: $\varepsilon_\infty = 3$, $\varepsilon_S = 50$, $\tau = 0.01$ s, $\omega_r = \frac{1}{\tau} = 100$ rad/s.

the following parameters were assumed $\varepsilon_\infty = 3$, $\varepsilon_S = 50$, $\tau = 0.01$ s, $\omega_r = \frac{1}{\tau} = 100$ rad/s. At low frequencies, the real part is constant (ε_S) and the imaginary part is around zero. When the angular frequency is approaching the relaxation frequency, the real part (ε') goes down while the imaginary part (ε'') reaches the maximum. At high frequencies again, the imaginary part is around zero while the real part stabilises at the value of ε_∞.

Knowing the electric permittivity of liquid crystals [$\varepsilon'(\omega)$ and $\varepsilon''(\omega)$] *vs*. the angular frequency (ω), both parameters can be calculated: $\psi'(\omega) = \frac{\varepsilon'}{|\varepsilon^*|^2}$ and $\psi''(\omega) = \frac{\varepsilon''}{|\varepsilon^*|^2}$ *vs*. angular frequency. Knowing these parameters, the amplitude U_{Cam} of out-signal and the phase shift φ can be obtained [using (15)].

3.1. *Liquid crystal with low electric strength*

Let us now consider that U_{in}=10 V, and $\omega_{RC} = 1000$ rad/s. Relaxation time τ in the LC changes from 0.1 s to 0.0001 s. Additionally, $\varepsilon_S = 10$ and $\varepsilon_\infty = 3$ ($\delta\varepsilon = \varepsilon_S - \varepsilon_\infty = 7$) are assumed. It means that a nematic LC with the low electric strength ($\delta\varepsilon$) are shown in this case. The amplitude U_{Cam} and the phase shift φ of out-signal can be calculated using (15) at assumed parameters.

In Fig. 9, the amplitude of the out-voltage U_{Cam} *vs*. the angular frequency ω is presented. It can be seen that filling the capacitor C_0 with the LC always shifts left the plot $U_{C0am}(\omega)$. For the empty capacitor, the cut-off frequency is exactly $\omega_{RC} = 1000$ rad/s (plot *empty*). For the liquid crystal with a very long relaxation time (low relaxation

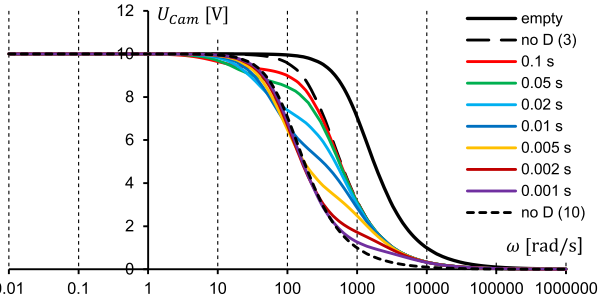

Fig. 9. Amplitude of out-voltage U_{Cam} *vs*. angular frequency ω (angular frequency in logarithmic scale). $U_{in} = 10$ V, $\omega_{RC} = 1000$ rad/s, $\varepsilon_S = 10$, and $\varepsilon_\infty = 3$. Relaxation times (shown in the legend) change from long [no D(3)] to short [no D(10)] values.

frequency), the cut-off frequency is ω_{co}=333 rad/s [plot no D(3)]. For the LC with a very short relaxation time (high relaxation frequency), the cut-off frequency is ω_{co} = 100 rad/s [plot no D(10)]. For intermediate values of relaxation time (assumed in the LC), it is difficult to define ω_{co}. For shorter relaxation times, the plots differ from plot no D(3) at lower frequencies while for higher frequencies, the plots of 0.1 s and 0.05 s (longer relaxation times) are identical to plot no D(3). For longer relaxation times, the plots differ from plot no D(10) at higher frequencies while for lower frequencies plots 0.002 s and 0.001 s (shorter relaxation times) are identical to plot no D(10).

Figure 10 seems to be more interesting. The normalized phase shift φ/π *vs*. the angular frequency ω is presented here. It can be seen that for the empty capacitor (plot empty), for cells filled with the LC exhibiting a very long relaxation time [plot no D(3)], and for cells filled with the LC showing a very short relaxation time [plot no D (10)], the phase shift φ *vs*. the angular frequency ω increases monotonically. For shorter relaxation times (shorter than 0.005 s), the plot φ *vs*. the angular frequency ω exhibits the local maximum at the angular frequency ω_{max}. It can also be seen that ω_{max} increases when the relaxation time decreases. Additionally, a local minimum can be observed at the angular frequency ω_{min}. Moreover, it is seen that ω_{min} increases when the relaxation time decreases. Phase shift φ/π for an empty capacitor reaches a value of 0.5 ($\varphi = \frac{\pi}{2}$ rad) practically at an angular frequency of 100 krad/s, while for a filled capacitor with the LC (τ = 0.0001 s), the phase shift φ/π reaches the value of 0.5 practically at an angular frequency of 1 mrad/s.

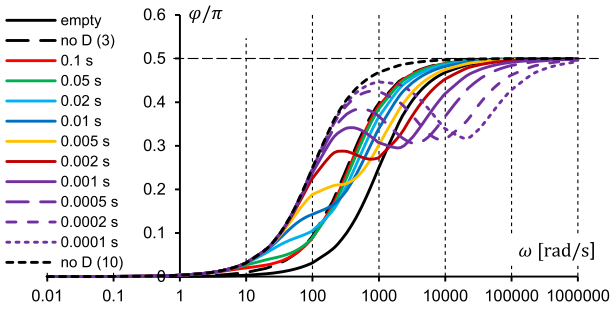

Fig. 10. Normalised phase shift φ/π *vs*. angular frequency ω (angular frequency in logarithmic scale). U_{in} = 10 V, ω_{RC} = 1000 rad/s, ε_S = 10, and ε_∞ = 3. Relaxation times (shown in the legend) change from long [no D(3)] to short [no D(10)] values.

In Figs. 11 and 12, two components of the amplitude U_{Cam} are shown respectively: in-phase component $U_{C(0)}$ and $-\frac{\pi}{2}$-phase component $U_{C\left(-\frac{\pi}{2}\right)}$. To calculate them, (11) was used. It means that $U_{C0(0)}$ is in phase with the external in-signal U_{in} while $U_{C0\left(-\frac{\pi}{2}\right)}$ lags the external in-signal by $\frac{\pi}{2}$ rad. In Fig. 13, plots of the $-\frac{\pi}{2}$-shifted component $[U_{C\left(-\frac{\pi}{2}\right)}]$ *vs*. the in-phase component $[U_{C(0)}]$ on the capacitor C_0 filled with LCs with different values of relaxation times are shown. U_{in} = 10 V, ω_{RC} = 1000 rad/s.

It is seen that the picture of the electric response of the RC filter is much more complicated for a capacitor filled with the LC with low dielectric strength than for an empty capacitor (Figs. 4–6).

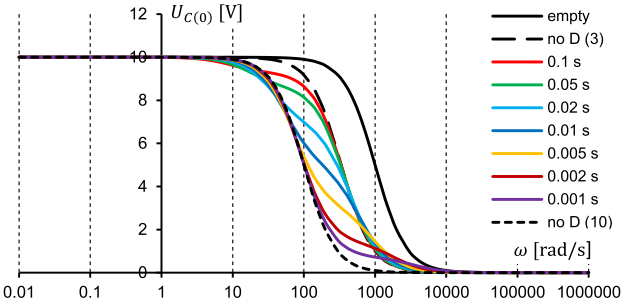

Fig. 11. Amplitude of in-phase $U_{C(0)}$ component of amplitude U_C of out-signal *vs*. angular frequency ω (angular frequency in logarithmic scale) for the capacitor filled with the LCs with different values of relaxation times (shown in the legend). U_{in} = 10 V, ω_{RC} = 1000 rad/s, ε_S = 10, and ε_∞ = 3.

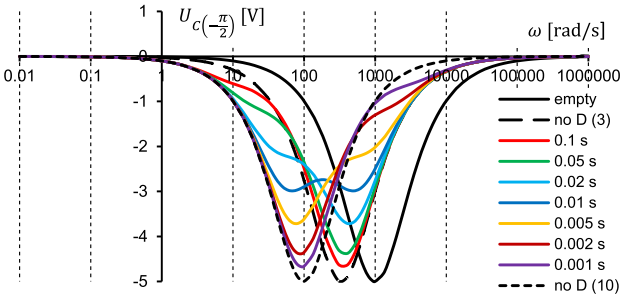

Fig. 12. Amplitude of $-\frac{\pi}{2}$-phase $U_{C\left(-\frac{\pi}{2}\right)}$ component of amplitude U_C of out-signal *vs*. angular frequency ω (angular frequency in logarithmic scale) for the cell filled with the LCs with different values of relaxation times (shown in the legend). U_{in} = 10 V, ω_{RC} = 1000 rad/s, ε_S = 10, and ε_∞ = 3.

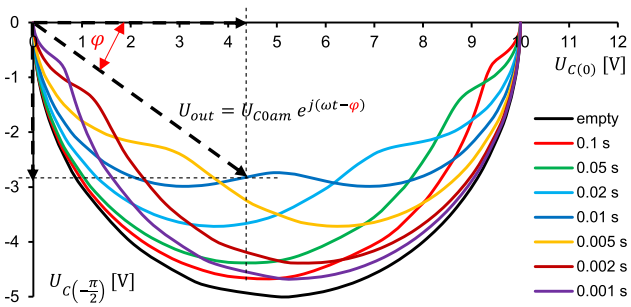

Fig. 13. $-\frac{\pi}{2}$-shifted component $(U_{C\left(-\frac{\pi}{2}\right)})$ *vs*. in-phase component $[U_{C(0)}]$ on capacitor C_0 filled with the LCs with different values of relaxation times (shown in the legend). U_{in} = 10 V, ω_{RC} = 1000 rad/s, ε_S = 10, and ε_∞ = 3.

3.2. *Liquid crystal with average electric strength*

Knowing the electric response for the RC filter with the capacitor filled with the LC with low electric strength ($\delta\varepsilon$ = 7), it can be assumed now that ε_S = 50 and ε_∞ = 3 ($\delta\varepsilon$ = 47 – average electric strength). Relaxation time τ in the LC changes from 1 s to 0.0001 s. As it was before: U_{in} = 10 V, and ω_{RC} = 1000 rad/s. Knowing these parameters, the amplitude U_{Cam} and the phase shift φ of out-signal can be calculated using (15) at assumed parameters.

In Fig. 14, the amplitude of out-voltage U_{Cam} *vs.* the angular frequency ω is presented. It can be seen that filling the capacitor C_0 with the LC with average electric strength shifts left the plot $U_{Cam}(\omega)$ in comparison with Fig. 9. For the empty capacitor, the cut-off frequency is exactly $\omega_{RC} = 1000$ rad/s (plot *empty*). For the LC with a very long relaxation time (low relaxation frequency), the cut-off frequency is $\omega_{co} = 333$ rad/s [plot no D(3)]. For the LC with a very short relaxation time (high relaxation frequency), the cut-off frequency is $\omega_{co} = 20$ rad/s [plot no D(50)]. For intermediate values of relaxation time (assumed in liquid crystal), it is difficult to define ω_{co}. For shorter relaxation times, the plots differ from plot no D(3) at lower frequencies, while for higher frequencies the plots of 1 s and 0.5 s (longer relaxation times) are identical to plot no D(3). For longer relaxation times, the plots differ from plot no D(50) at higher frequencies, while for lower frequencies, the plots of 0.005 s and 0.002 s (shorter relaxation times) are identical to plot no D(50). The frequency range of the electric response modification is wider than in the case of the LC with low dielectric strength.

Figure 15 seems to be more interesting. The normalized phase shift φ/π *vs.* the angular frequency ω is presented here. It can be seen that for the empty capacitor (plot *empty*), for cells filled with the LC showing a very long relaxation time [plot no D(3)], and for cells filled with the LC exhibiting a very short relaxation time [plot no D(50)], the phase shift φ *vs.* the angular frequency ω increases monotonically. For capacitors filled with the LC showing average relaxation times, the plot φ *vs.* the angular frequency ω exhibits the local maximum at the angular frequency ω_{max}. It can be observed that ω_{max} increases when the relaxation time decreases. Additionally, a local minimum can be observed at the angular frequency ω_{min}. And again, ω_{min} increases when the relaxation time decreases. Phase shift φ/π for an empty cell reaches a value of 0.5 ($\varphi = \frac{\pi}{2}$ rad) practically at an angular frequency of 100 krad/s. For a filled capacitor with the LC ($\tau = 0.0001$s), the phase shift φ/π reaches a value of 0.5 practically at an angular frequency of 10 mrad/s. It is seen (Fig. 15) that the modulation depth of φ is larger in this case than for the liquid crystal with low electric strength (Fig. 10).

In Figs. 16 and 17, two components of the amplitude U_{Cam} are shown respectively: in-phase component $U_{C(0)}$ and $-\frac{\pi}{2}$-phase component $U_{C\left(-\frac{\pi}{2}\right)}$. To calculate them, (11) was used. It means that $U_{C0(0)}$ is in phase with the external in-signal U_{in} while $U_{C0\left(-\frac{\pi}{2}\right)}$ lags the external in-signal by $\frac{\pi}{2}$ rad.

In Fig. 18, plots of the $-\frac{\pi}{2}$-shifted component $[U_{C\left(-\frac{\pi}{2}\right)}]$ *vs.* the in-phase component $[U_{C(0)}]$ on the capacitor C_0 filled with the LCs with different values of relaxation times are shown. $U_{in} = 10$ V, $\omega_{RC} = 1000$ rad/s. It is observed that the picture of the electric response of the RC filter is much more complicated for the capacitor filled with the LC medium with average dielectric strength than for the empty

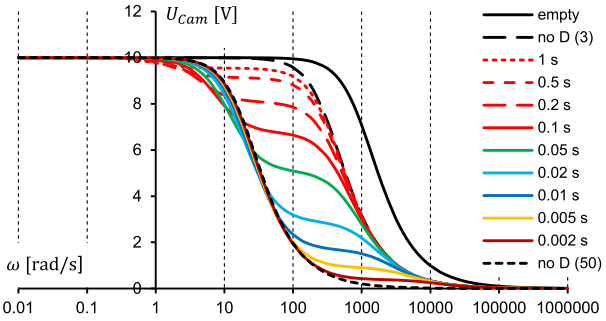

Fig. 14. Amplitude of out-voltage U_{Cam} *vs.* angular frequency ω (angular frequency in logarithmic scale). $U_{in} = 10$ V, $\omega_{RC} = 1000$ rad/s, $\varepsilon_S = 50$, and $\varepsilon_\infty = 3$. Relaxation times (shown in the legend) change from long [no D(3)] to short [no D(50)] values.

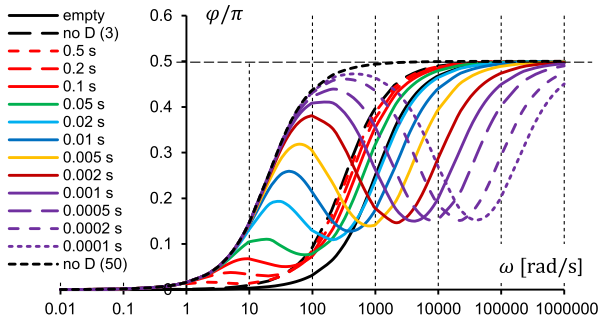

Fig. 15. Normalised phase shift φ/π *vs.* angular frequency ω (angular frequency in logarithmic scale). $U_{in} = 10$ V, $\omega_{RC} = 1000$ rad/s, $\varepsilon_S = 50$, and $\varepsilon_\infty = 3$. Relaxation times (shown in the legend) change from long [no D(3)] to short [no D(50)] values.

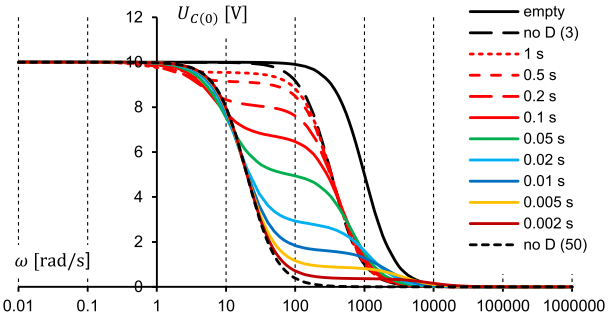

Fig. 16. Amplitude of in-phase $U_{C0(0)}$ component of amplitude U_{Cam} of out-signal *vs.* angular frequency ω (angular frequency in logarithmic scale) for the cell filled with the LCs with different values of relaxation times (shown in the legend). $U_{in} = 10$ V, $\omega_{RC} = 1000$ rad/s, $\varepsilon_S = 50$, and $\varepsilon_\infty = 3$.

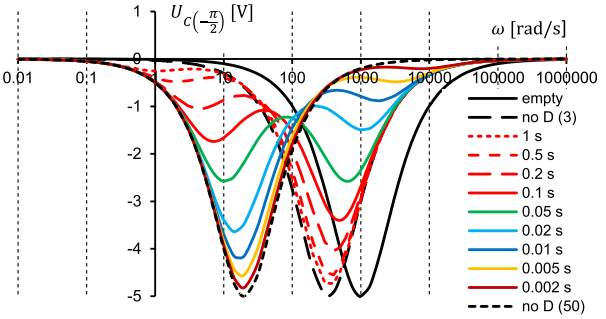

Fig. 17. Amplitude of $-\frac{\pi}{2}$-phase $U_{C\left(-\frac{\pi}{2}\right)}$ component of amplitude U_{Cam} of out-signal *vs.* angular frequency ω (angular frequency in logarithmic scale) for the cell filled with the LCs with different values of relaxation

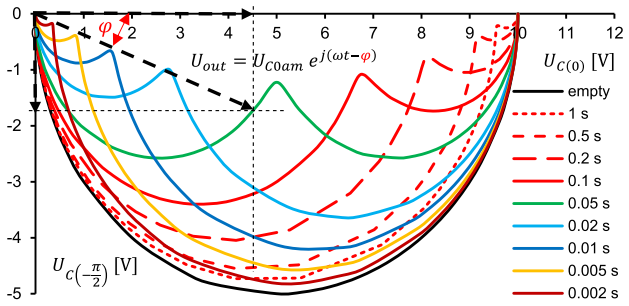

Fig. 18. $-\frac{\pi}{2}$-shifted component $[U_{C(-\frac{\pi}{2})}]$ *vs.* in-phase component $[U_{C(0)}]$ on capacitor C_0 filled with the LCs with different values of relaxation times (shown in the legend). $U_{in} = 10$ V, $\omega_{RC} = 1000$ rad/s, $\varepsilon_S = 50$, and $\varepsilon_\infty = 3$.

capacitor (Fig. 6), as well as for the capacitor filled with the LC medium with low dielectric strength (Fig. 13).

3.3. *Liquid crystal with high electric strength*

Knowing the electric response for the RC filter with the capacitor filled with the LC with average electric strength ($\delta\varepsilon = 47$), it can be assumed now that $\varepsilon_S = 100$ and $\varepsilon_\infty = 3$ ($\delta\varepsilon = 97$ – high electric strength). Relaxation time τ in the LC changes from 2 s to 0.0001 s. As it was before: $U_{in} = 10$ V and $\omega_{RC} = 1000$ rad/s. Knowing these parameters, the amplitude U_{Cam} can be calculated at the phase shift φ of out-signal using (15).

In Fig. 19, the amplitude of the out-voltage U_{Cam} *vs.* the angular frequency ω is presented. It is seen that filling the capacitor C_0 with the LC with high electric strength shifts left the plot $U_{Cam}(\omega)$ in comparison with Fig. 14. For the empty capacitor, the cut-off frequency is exactly $\omega_{RC} = 1000$ rad/s (plot empty). For the LC with a very long relaxation time (low relaxation frequency), the cut-off frequency is $\omega_{co} = 333$ rad/s [plot no D(3)]. For the LC with a very short relaxation time (high relaxation frequency), the cut-off frequency is $\omega_{co} = 10$ rad/s [plot no D(100)]. For intermediate values of relaxation time (assumed in the liquid crystal), it is difficult to define ω_{co}. For shorter relaxation times, the plots differ from plot no D(3) at lower frequencies while for higher frequencies plots of 2 s and 1 s (longer relaxation times) are identical to plot no D(3). For longer relaxation times, the plots differ from plot no D(100) at higher frequencies while for lower frequencies plots of 0.005 s, 0.01 s, and 0.02 s (shorter relaxation times) are identical to plot no D(100). The frequency range of the electric response modification is wider than in the case of the LC with average and low dielectric strength.

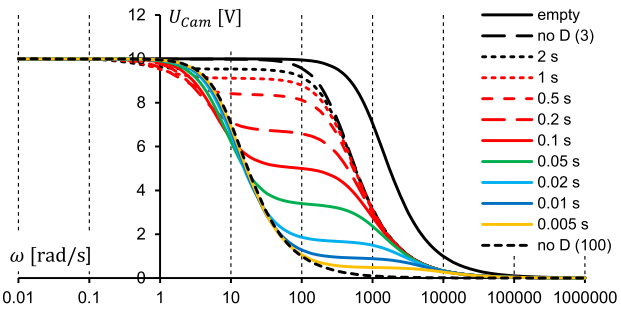

Fig. 19. Amplitude of out-voltage U_{Cam} *vs.* angular frequency ω (angular frequency in logarithmic scale). $U_{in} = 10$ V, $\omega_{RC} = 1000$ rad/s, $\varepsilon_S = 100$, and $\varepsilon_\infty = 3$. Relaxation times (shown in the legend) change from long [no D(3)] to short [no D(100)] values.

Figure 20 seems to be more interesting. The normalized phase shift φ/π *vs.* the angular frequency ω is presented here. It can be seen that for the empty capacitor (plot *empty*), for cells filled with a liquid crystal showing a very long relaxation time [plot no D(3)], and for cells filled with a liquid crystal showing a very short relaxation time [plot no D(100)], the phase shift φ *vs.* the angular frequency ω increases monotonically. For cells filled with the LC for average relaxation times, the plot φ *vs.* angular frequency ω exhibits the local maximum at the angular frequency ω_{max}. It is seen that ω_{max} increases when the relaxation time decreases. Additionally, the local minimum at the angular frequency ω_{min} can be observed. Moreover, it can be noticed that ω_{min} increases when the relaxation time decreases. Phase shift φ/π for an empty cell reaches a value of 0.5 ($\varphi = \frac{\pi}{2}$ rad) practically at an angular frequency of 100 krad/s, while for a filled cell with a liquid crystal ($\tau = 0.0001$ s), the phase shift φ/π reaches a value of 0.5 practically at an angular frequency around 100 mrad/s. It is seen that the modulation depth of φ is larger in this case than for the LC with average electric strength (Fig. 15).

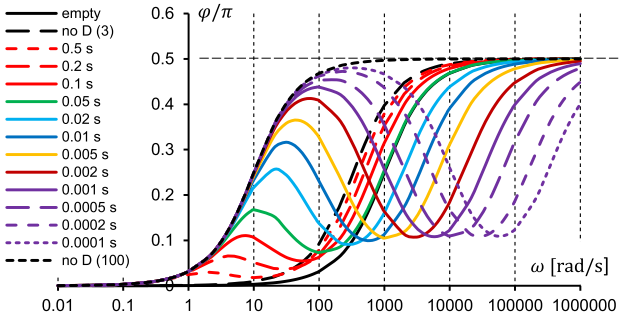

Fig. 20. Normalised phase shift φ/π *vs.* angular frequency ω (angular frequency in logarithmic scale). $U_{in} = 10$ V, $\omega_{RC} = 1000$ rad/s, $\varepsilon_S = 100$, and $\varepsilon_\infty = 3$. Relaxation times (shown in the legend) change from long [no D(3)] to short [no D(100)] values.

In Figs. 21 and 22, two components of the amplitude U_{Cam} are shown respectively: in-phase component $U_{C(0)}$ and $-\frac{\pi}{2}$-phase component $U_{C(-\frac{\pi}{2})}$. Equation (11) was used to calculate them. It means that $U_{C0(0)}$ is in phase with the external in-signal U_{in} while $U_{C0(-\frac{\pi}{2})}$ lags the external in-signal by $\frac{\pi}{2}$ rad. In Fig. 23, plots of $-\frac{\pi}{2}$-shifted component $[U_{C(-\frac{\pi}{2})}]$ *vs.* the in-phase component $[U_{C(0)}]$ on the capacitor C_0 filled with the LCs with different values of relaxation times are shown. $U_{in} = 10$ V, $\omega_{RC} = 1000$ rad/s. The picture of the electric response of the RC filter is much more complicated for the capacitor filled with the LC medium with high dielectric strength than for the empty capacitor (Fig. 6), as well as the capacitor filled with the LC medium with low (Fig. 13) and average (Fig. 18) dielectric strength.

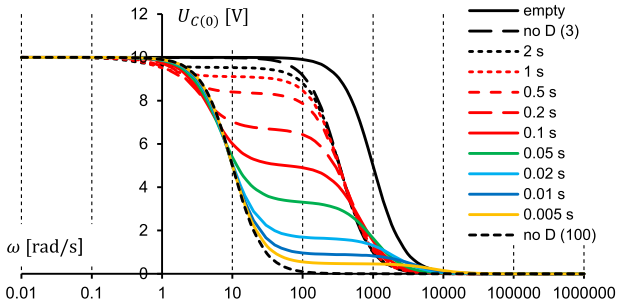

Fig. 21. Amplitude of in-phase $U_{C0(0)}$ component of amplitude U_{Cam} of out-signal *vs*. angular frequency ω (angular frequency in logarithmic scale) for the cell filled with the LC with different values of relaxation times (shown in the legend). $U_{in} = 10$ V, $\omega_{RC} = 1000$ rad/s, $\varepsilon_S = 100$, and $\varepsilon_\infty = 3$.

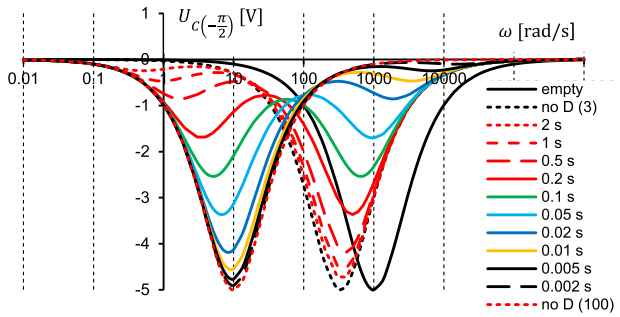

Fig. 22. Amplitude of $-\frac{\pi}{2}$-phase $U_{C(-\frac{\pi}{2})}$ component of amplitude U_{Cam} of out-signal *vs*. angular frequency ω (angular frequency in logarithmic scale) for the cell filled with the LC with different values of relaxation times (shown in the legend). $U_{in} = 10$ V, $\omega_{RC} = 1000$ rad/s, $\varepsilon_S = 100$, and $\varepsilon_\infty = 3$.

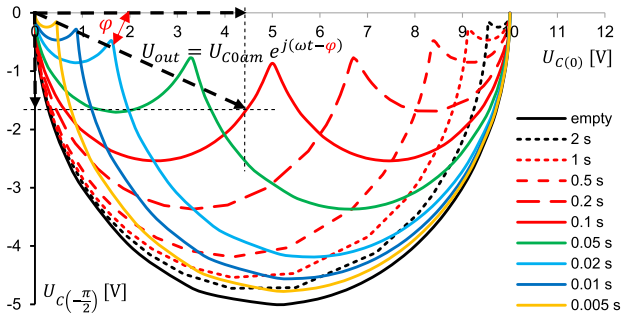

Fig. 23. $-\frac{\pi}{2}$-shifted component $[U_{C(-\frac{\pi}{2})}]$ *vs*. in-phase component $[U_{C(0)}]$ on capacitor C_0 filled with the LCs with different values of relaxation times (shown in the legend).

4. Conclusions

When the results shown in Figs. 2–6 obtained for the empty cell are compared with the results shown in Figs. 9–13, in Figs. 14–18, and in Figs. 19–23 obtained for nematic LC with low electric strength ($\delta\varepsilon = 7$), with average electric strength ($\delta\varepsilon = 47$) and with high electric strength ($\delta\varepsilon = 97$) respectively, it can be concluded that the LC with different electric strength significantly modifies the electric response of the low-pass RC filter. It is not only related to a shift of the electric response into the lower frequency range, but also the phase shift φ starts to change non-monotonically (in contrast to a classical low-pass RC filter).

Equations (11) and (15) derived in this paper describe the properties of the low-pass RC filter for any electric properties of the LC. The cases presented in this paper are the simplest ones. Only one Debye relaxation is assumed, and any additional effects are not taken into account. It is worth stressing that the effect considered in this paper can be more complicated. For example, two relaxations could be presented in the analysed LC. Not only Debye relaxation but also Cole-Cole, Cole-Davisson, or Havriliak-Negami ones can be considered in the analysed medium. The relaxations observed in the LCs usually depend on temperature. When the temperature increases, the relaxation frequency usually increases according to the Arrhenius law. Additionally, it can be assumed that nematic LCs can be reoriented using an electric field with the proper frequency and strength. This reorientation called the Fréedericksz transition is triggered by the electric anisotropy $\Delta\varepsilon$ of the aligned nematic phase. For the reorientation, an electric field existing in the capacitor in a low-pass RC filter can be used. The reorientation in the capacitor makes the LC a completely different medium from an electric point of view. This makes the potential influence of LC properties on the low-pass RC filter properties richer than shown in this paper. Additionally, the electric strength analysed in this paper is limited to 100. It seems that for a typical nematic LC, it is the highest possible value [13]. But the discovery of ferroelectricity in nematics [14–18] shifts this limit even to 8000. This can expand the application of LCs also as dielectric materials for electronics.

Acknowledgements

This work was sponsored by Military University of Technology grant no. UGB 22-793 (funds for 2022).

References

[1] *Relaxation Phenomena.* (eds. Wróbel, S & Haase, W) (Springer-Verlag Berlin, 2003). https://doi.org/10.1007/978-3-662-09747-2

[2] Dunmur, D. & Toriyama, K. Dielectric propreties in *Physical properties of liquid crystals* (eds. Demus, D., Goodby, J., Gray, G. W., Spiess, H. W. & Vill, V.) 129–150 (Wiley-VCH Weinheim, 1999)

[3] Lagerwall, S. T. *Ferroelectric and Antiferroelectric Luquid Crystals*. (Wiley-VCH Weinheim 1999)

[4] Buivydas, M. *et al*. Collective and non-collective excitations in antiferroelectric and ferrielectric liquid crystals studied by dielectric relaxation spectroscopy and electro-optic measurements. *Liq. Cryst*. **23**, 723–739 (1997). https://doi.org/10.1080/026782997208000

[5] Holtzer, A. M. *The Collected Papers of Peter J. W. Debye*. (Interscience, New York – London, 1954). https://doi.org/10.1002/pol.1954.120137203

[6] Cole, K. S. & Cole, R. H. Dispersion and absorption in dielectrics. Alternating current characteristics. *J. Chem. Phys*. **9**, 341–351 (1941). https://doi.org/10.1063/1.1750906

[7] Davidson, D. W. & Cole, R. H. Dielectric relaxation in glycerol, propylene glycol and n-propanol. *J. Chem. Phys*. **19**, 1484–1491 (1951). https://doi.org/10.1063/1.1748105

[8] Havriliak, S. & Negami, S. A complex plane representation of dielectric and mechanical relaxation processes in some polymers. *Polymer* **8**, 161–210 (1967). https://doi.org/10.1016/0032-3861(67)90021-3

[9] Perkowski, P. Dielectric spectroscopy of liquid crystals. Theoretical model of ITO electrodes influence on dielectric measurements.

Opto-Electron. Rev. **17**, 180–186 (2009). https://doi.org/10.2478/s11772-008-0062-8

[10] Perkowski, P. Dielectric spectroscopy of liquid crystals. Electrodes resistivity and connecting wires inductance influence on dielectric measurements, *Opto-Electron. Rev*. **20**, 79–86 (2012). https://doi.org/10.2478/s11772-012-0004-3

[11] Perkowski, P. The parasitic effects in high-frequency dielectric spectroscopy of liquid crystals – the review. *Liq. Crys.* **48**, 767–793 (2021). https://doi.org/10.1080/02678292.2020.1852619

[12] Fréedericksz, V. & Repiewa, A. Theoretisches und Experimentelles zur Frage nach der Natur der anisotropen Flüssigkeiten. *Zeitschrift für Physik* **42**, 532–546 (1927). https://doi.org/10.1007/BF01397711 [in German]

[13] Mrukiewicz, M., Perkowski, P., Strzeżysz, O., Węgłowska, D. & Piecek. W. Pretransitional effects in a mesogenic mixture under an electric field, *Phys. Rev. E*. **97**, 052704 (2018). https://doi.org/10.1103/PhysRevE.97.052704

[14] Li, J. *et al*. Development of ferroelectric nematic fluids with giant-ε dielectricity and nonlinear optical properties. *Sci. Adv*. **7**, abf5047 (2021). https://doi.org/10.1126/sciadv.abf5047

[15] Chen, X., Korblova, E., Dong, D. & Clark, N. A. First-principles experimental demonstration of ferroelectricity in a thermotropic nematic liquid crystal: Polar domains and striking electro-optics. *Proc. Natl. Acad. Sci. USA* (*PNAS)* **117**, 14021–14031 (2020). https://doi.org/10.1073/pnas.2002290117

[16] Mandle, R. J., Cowling, S. J. & Goodby, J. W. Rational design of rod-like liquid crystals exhibiting two nematic phases. *Chem. Eur. J.* **23**, 14554–14562 (2017). https://doi.org/10.1002/chem.201702742

[17] Mandle, R. J., Cowling, S. J. & Goodby, J. W. A nematic to nematic transformation exhibited by a rod-like liquid crystal. *Phys. Chem. Chem. Phys*. **19**, 11429–11435 (2017). https://doi.org/10.1039/C7CP00456G

[18] Sebastián, N. *et al*. Ferroelectric-ferroelastic phase transition in a nematic liquid crystal. *Phys. Rev. Lett.* **124**, 037801 (2020). https://doi.org/10.1103/PhysRevLett.124.037801